European Review for Medical and Pharmacological Sciences 2019; 23: 1184-1195

Attenuating the abnormally high expression of AEBP1 suppresses the pathogenesis of childhood acute lymphoblastic leukemia via p53-dependent signaling pathway

S. LI[1,2], C.-X. JUAN[1], A.-M. FENG[2] , H.-L. BIAN[2], W.-D. LIU[2], G.-Q. ZHANG[2], C.-Z. WANG[2], Q. CAO[1], G.-P. ZHOU[1]

[1]Department of Pediatrics, The First Affiliated Hospital of Nanjing Medical University, Nanjing, China
[2]Department of Pediatrics, Yancheng Maternity and Child Health Care Hospital, Yancheng, China

Abstract. – OBJECTIVE: This study aimed to explore the candidate genes and their potential mechanism in childhood acute lymphoblastic leukemia (cALL).

MATERIALS AND METHODS: Differentially expressed genes (DEGs) were screened from GSE67684 (treatment), GSE28460 (relapse), and GSE60926 (relapse). The expression of AEBP1 at different stages of cALL was analyzed followed by functional enrichment analysis of its co-expressed genes. Expression of AEBP1 was determined in different leukemia cell lines and knocked down in Jurkat cells. Cell behaviors as well as the expression of p53, Bax, and Bcl-2 were also evaluated after silencing AEBP1 in Jurkat cells.

RESULTS: Two clusters: Profile 1 (downward) and Profile 26 (upward) were identified in GSE67684, and 53 Profile 1-specific DEGs were identified compared with DEGs in GSE28460 and GSE60926. AEBP1 was one of these genes and was significantly downregulated after treatment but upregulated in relapse samples. Functional enrichment analysis revealed that AEBP1 co-expressed genes were significantly enriched in GO terms including immune response, blood coagulation etc. and in the hematopoietic cell lineage and PI3K/Akt signaling pathways. AEBP1 was significantly increased in leukemia cell lines, especially in Jurkat cells, compared with the Pbmc cells. Silencing AEBP1 markedly reduced proliferation and induced cell cycle arrest in Jurkat cells, but also promoted apoptosis of Jurkat cells. Silencing AEBP1 also inhibited the expression of p53 and Bcl-2 but promoted Bax in Jurkat cells.

CONCLUSIONS: AEBP1 was highly-expressed in the diagnosis and relapse cALL, and silencing AEBP1 significantly reduced proliferation but promoted apoptosis in Jurkat cells via a p53-dependent pathway.

Key Words:
Childhood acute lymphoblastic leukemia, AEBP1, Proliferation, Apoptosis, Cell cycle, p53.

Introduction

Childhood acute lymphoblastic leukemia (cALL) is the most common malignancy in children and adolescents, and is one of the leading causes of mortality in childhood[1,2]. It is estimated that at least 54,000 new cases of cALL are diagnosed in Asia annually[3]. With the development of medical technologies, although 80% of cALL cases can be cured by application of modern treatment, 20% undergo relapse despite receiveing appropriate treatments[4,5]. Therefore, it is important to further explore the pathogenesis of cALL to improve the understanding, diagnosis, and treatment of cALL. In recent decades, development of high-throughput sequencing has provided a new method to elucidate the mechanism of cALL. Exome sequencing revealed that CNOT3 and the ribosomal genes RPL5 and RPL10 were mutated in T-cell ALL, indicating that ribosome might be an underlying oncogenic factor[6]. A whole genome sequencing based on 15 Philadelphia chromosome-positive (Ph-like) ALL cases revealed that the ABL1, JAK2, PDGFRB, and CELF2 were rearranged and that IL7R and FLT3 were abnormally activated in ALL, which will induce transformation and could be attenuated by tyrosine kinase inhibitors[7]. A genome-wide association study of 511 ALL cases and 6661 non-ALL controls documented that inherited *GAT3*

Corresponding Author: Guoping Zhou, MD; e-mail: guopzhou2018@163.com

variants are associated with the pathogenesis and relapse of Ph-like cALL, but the exact mechanism of *GAT3* in cALL remains unclear[8]. In addition, exome sequencing has revealed that the activating mutation of *STAT5B* is a common abnormality in pediatric T-cell ALL and significantly associated with a higher rate of relapse[9]. However, how these mutations work in the pathogenesis of ALL, including cALL, is still not fully understood or confirmed by experiments. In the current study, three microarray datasets provided by the Gene Expression Ominous (GEO, https://www.ncbi.nlm.nih.gov/geo/) were systematic secondarily mined to identify promising candidate genes associated with cALL, and the results indicated that adipocyte enhancer-binding protein 1 (AEBP1) was significantly correlated with the pathogenesis and relapse of cALL. In addition, functional enrichment predication and molecular experiments were also performed to validate our findings. Based on these investigations, we hope to provide useful insights into understanding, diagnosis, and treatment of cALL.

Materials and Methods

Data Sourcing

Three cALL datasets GSE67684 (https://www.ncbi.nlm.nih.gov/geo/query/acc.cgi?acc=GSE67684), GSE28460, and GSE60926 were downloaded from the GEO database and used for the following investigations. Specifically, GSE67684 contains 495 children cALL samples, including 194 in the Day0 group (diagnosed), 193 in the Day8 group (underwent treatment for 9 days), 49 in the Day15 group (underwent treatment for 15 days), and 59 in the Day33 group (underwent treatment for 33 days). GSE28460 includes 49 diagnosis and 49 relapse children cALL samples, and GSE60926 contains 22 diagnosis cALL samples and 20 relapse children cALL samples. These three datasets were sequenced on the platform of GPL570 [HG-U133_Plus_2] Affymetrix Human Genome U133 Plus 2.0 Array. Following this, expression console was used to obtain the expression information of probes in each dataset.

Identification of DEGs and Venn Analysis

According to the probe expression information, DEGs of time series in GSE67684 were screened using the Fisher test with the thresholds of a random variance model (RVM) of adjust p-value ≤ 0.05 and a false discovery rate (FDR) ≤ 0.05. Based on the isolated DEGs, the expression trends of these DEGs were analyzed using series test of cluster (STC) according to the treatment time point: Day0→Day8→Day15→Day33. DEGs between the diagnosis and relapse samples in GSE28460 and GSE60926 were identified using the small variance of the RVM model with the thresholds of $p \leq 0.05$ and fold changes (FC) >1.2. Following this, a Venn diagram was used to isolated time series specific DEGs.

Expression of AEBP1 in Different Stages of cALL

To further reveal the value of AEBP1, the expression of AEBP1 in each stage of cALL in the three datasets (GSE67684, GSE28460, and GSE60926) was calculated using ggplot2 package in R.

AFBP1 Co-Expressed Gene Expression and Functional Enrichment

According to the DEGs identified in GSE67684, AEBP1 co-expressed DEGs were analyzed using the Pearson co-efficient. Following this, the top 200 co-expressed DEGs were subjected to functional enrichment analysis based on the annotation in the Gene Ontology (GO) and Kyoto Encyclopedia of Genes and Genomes (KEGG) databases. Significant enrichment was considered when $p<0.05$ and FDR <0.05. Following this, the AEBP1-gene-pathway regulatory network for the top 200 co-expressed genes was established using Cytoscape 3.2.0.

Cell Culture

In this study, the lymphoma cell lines: Jurkat, Nalm-6, and Raji, and the normal cell line 293T were cultured for the following experimental investigations. Specifically, Jurkat, and Raji cells were maintained in Roswell Park Memorial Institute-1640 (RPMI-1640) medium (Gibco, Carlsbad, CA, USA) containing 10% fetal bovine serum (FBS, Gibco, Rockville, MD, USA) and 1% penicillin-streptomycin (Sigma-Aldrich, St. Louis, MO, USA) and 293T cells were maintained in Dulbecco's Modified Eagle Medium (DMEM) (Gibco, Rockville, MD, USA) containing 10% fetal bovine serum (FBS) and 1% penicillin-streptomycin. In addition, peripheral blood mononuclear cells (PBMCs) were isolated from the serum of a healthy control using a Ficoll-Paque Plus (TBDscience, Tianjin, China) density gradient centrifugation and maintained in RPMI-1640 medium containing 10% fetal bovine serum (FBS) and 1% penicillin-streptomycin. All

cells were kept in a humidity incubator at 37°C with a 5% CO_2 atmosphere.

Construction of shAEBP1 Lentivirus

According to the accession number of AEBP1 in PubMed, the shRNA sequence of AEBP1 was designed, and a non-significant sequence was used as a negative control. Following this, the shAEBP1 plasmid was constructed by Shanghai Genechem CO., Ltd., (Shanghai, China). Subsequently, shNC or shAEBP1, pHelper 1.0 and pHelper 2.0 were co-transfected into 293T cells using lipofectamine 2000 (Invitrogen, Carlsbad, CA, USA) according to the manufacturer's protocol. After transfection for 48 h, supernatants of 293T cells were harvested to infect 70% confluency of Jurkat cells. Following 72 h of infection, Jurkat cells were harvested for knocked down confirmation and the following investigation.

Flow Cytometry

Cell cycle and apoptosis were determined using flow cytometry. Briefly, cells were seeded in a 6-cm dish overnight to a confluency of 80%. Then, cells were typsinzed, washed with pre-cooled D-Hanks (pH = 7.2~7.4), and fixed with 75% ethanol at 4°C for 1 h. Following this, cells were stained with propidium iodide (PI) solution (PI 50 μg/mL and RNase A 200 μg/mL, Sigma-Aldrich, St. Louis, MO, USA) at room temperature for 30 min in the dark and analyzed using a Guava®easyCyte™8HT flow cytometer (Millipore, Billerica, MA, USA). Each experiment was performed in triplicate and the average value was calculated as the final result.

Cell Counting Kit-8 (CCK-8) Assay

After silencing shAEBP1, control or shAEBP1 cells were seeded in 96-well plates at a density of 2.0×10^3 cells per well. Each sample was repeated five times. Then, cell proliferation was determined using CCK-8 (Sigma-Aldrich, St. Louis, MO, USA) for five days after seeding. Briefly, CCK-8 solution was added to each well and incubated at 37°C for 4 h according to the manufacturer's protocol. Following this, the optical density (OD) value at 450 nm was determined using a microplate reader (Tecan Infinite, Männedorf, Switzerland).

Quantitative Real-Time Polymerase Chain Reaction (RT-qPCR)

Following treatment, total RNA in cells was isolated using TRIzol reagent (Shanghai Pufei, Shanghai, China) and reversed transcribed into complementary deoxyribose nucleic acid (cDNA) using Promega M-MLV (Promega, Madison, WI, USA) according to the manufacturer's protocols. Next, the amplification of genes was performed using 6.0 μL of SYBR Master Mixture (TaKaRa, Otsu, Shiga, Japan), 0.3 μL of 5 μM primer mix, 0.6 μL of template (cDNA), and 5.1 μL of RNase-free H_2O with the following condition: 95°C for 30 s and 40 cycles of 95°C for 5 s and 60°C for 30 s in a Real-time PCR instrument (Roche, Basel, Switzerland). Primers for these genes were designed as follows: AEBP1: forward, 5'-CAGCATCCATGACGATTTTGT-3' and reverse, 5'-CATTCCAGGTGAGTGGGTAGAT-3'; and GAPDH (internal control): forward, 5'-TGACTTCAACAGCGACACCCA-3' and reverse, 5'-CACCCTGTTGCTGTAGCCAAA-3'. Relative gene expression was analyzed using the $2^{-\Delta\Delta Ct}$ method[6].

Western Blotting

After treatment, cells were lysed with radioimmunoprecipitation assay (RIPA) lysis buffer (Beyotime, Shanghai, China) containing a cocktail of proteases inhibitors (Beyotime, Shanghai, China). Then, cells were harvested and centrifuged at 4°C, 10,000 g. The supernatants were collected and quantified using the BCA method (BCA Protein Assay Kit, Beyotime, Shanghai, China). After boiling with an equal volume of loading buffer, protein solutions were subjected to sodium dodecyl sulphate-polyacrylamide gel electrophoresis (SDS-PAGE) and transferred to a polyvinylidene difluoride (PVDF) membrane (Millipore, Billerica, MA, USA). After that, the membranes were blocked with a 5% skim milk solution at room temperature for 1 h and incubated with primary mouse anti-AEBP1 (1:300, Santa Cruz, Santa Cruz, CA, USA), mouse anti-p53 (1:1000, Cell Signaling Technology, Danvers, MA, USA), mouse anti-Bcl-2 (1:500, Abcam, Cambridge, MA, USA), rabbit anti-Bax (1:1000, Abcam), or mouse anti-GAPDH (1:2000, Santa Cruz, Santa Cruz, CA, USA) at 4°C overnight. After washing with Tris buffered saline and Tween 20 (TBST) for 8 min × 4 times, the membranes were incubated with mouse anti-rabbit or rabbit anti-mouse antibody (1:5000, Santa Cruz, Santa Cruz, CA, USA) at room temperature for 1.5 h. After rinsing with TBST for 8 min × 4 times, the blots membranes were visualized using the enhanced chemiluminescence method (Pierce, Rockford, IL, USA).

Statistical Analysis

Statistical analyses were performed using GraphPad Prism 6.0 (GraphPad Software, La Jolla, CA, USA). Continuous variables are presented with the mean ± standard deviation (SD) and comparisons between groups were estimated using Student's *t*-test. For all comparisons, $p<0.05$ was considered to be statistically significant.

Results

DEGs Identification and Clustering

According to the thresholds, a total of 1621 DEGs were identified in the GSE67684 dataset between 0day and other treatment days. After clustering using STC, eight significant changed gene profiles were identified (Figure 1). Specifically, Profile 1 was the only downward gene profile and Profile 26 was the only upward gene profile among these significantly changed gene profiles (Figure 2A). Moreover, a total of 1529 DEGs were identified in GSE28460, including 570 upregulated genes and 959 downregulated genes. In addition, 1012 DEGs were identified in GSE60929, including 407 upregulated genes and 605 downregulated genes. A Venn diagram was performed for the DEGs in Profile 1, GSE28460, and GSE60929 to screen cALL treatment associated genes. As a result, 53 DEGs were identified to be specifically included in Prolife1, including AEBP1, ALDH5A1, ATF3, AUTS2, BAALC, BCL7A, BICD1, CLEC14A, CRIM1, CTGF, etc. (Figure 2B).

Expression of AEBP1 in Different Stages of cALL

The aforementioned results indicated that AEBP1 might play critical roles in the treatment

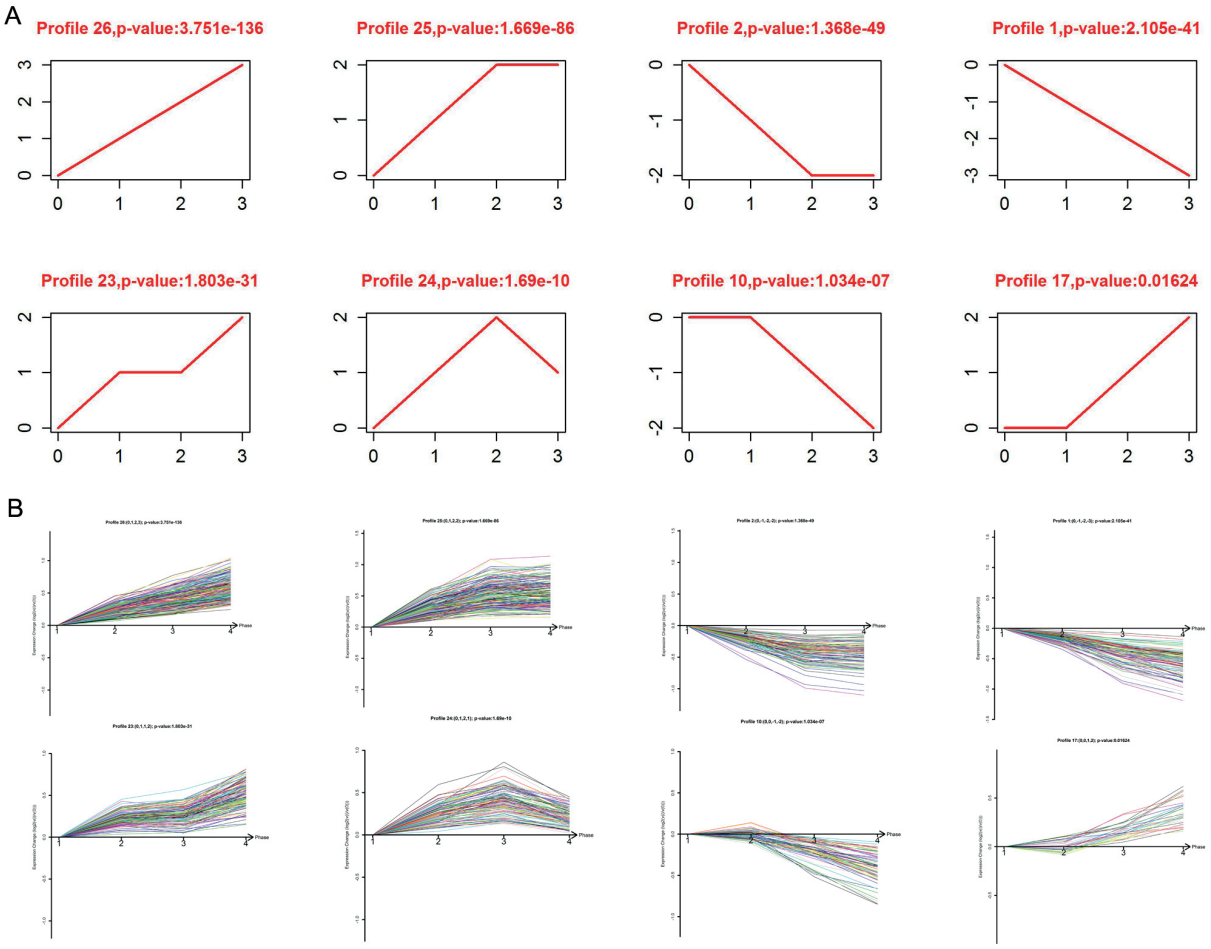

Figure 1. Expression trends of DEGs identified in GSE67684. ***A***, Expression trends of DEG profiles followed by the diagnosis of Day0-Day8-Day15-Day33; ***B***, Expression characteristics of DEGs with similar variation tendency. DEGs: differentially expressed genes.

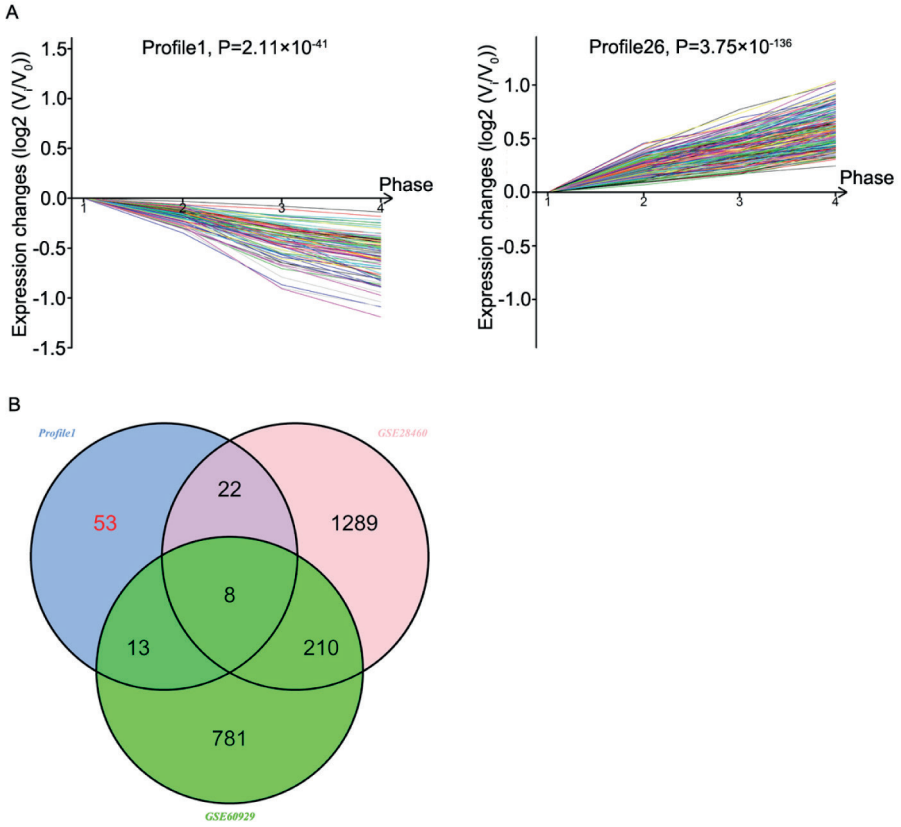

Figure 2. DEGs identified in GSE67684, GSE28460, and GSE60926. ***A,*** Significantly downward and upward gene cluster in GSE67684; ***B,*** Venn analysis among profile 1 in GSE67684, GSE28460, and GSE60926. DEGs: differentially expressed genes.

of cALL. Therefore, the change in expression of AEBP1 in different stages was explored according to the probe information included in the three datasets GSE67684, GSE28460, and GSE60929. The result indicated that expression of AEBP1 was significantly downregulated after treatment in a time-dependent manner but there was no signifcant difference between the diagnosed and relapse groups (Figure 3). These findings suggested that AEBP1 might play critical roles in the treatment of cALL and could serve a promising biomarker for the prognosis of cALL treatment.

Functional Enrichment Analysis for AEBP1 Co-Expressed Genes

The top 200 AEBP1 co-expressed genes were isolated from GSE67684 using the Pearson co-efficient. Then, functional enrichment analyses were conducted for these co-expressed genes. GO functional enrichment analysis revealed that these co-expressed genes were significantly enriched in the terms of immune response (p=2.73×10^{-18}), blood coagulation (p=1.31×10^{-13}), platelet degranulation (p=7.65×10^{-13}), inflammatory response (p=6.65×10^{-12}), and cell adhesion (p=1.50×10^{-11}) (Table I). The KEGG pathway analysis demonstrated that the co-expressed genes were significantly enriched in 57 pathways, including hematopoietic cell lineage (p=1.22×10^{-13}), cytokine-cytokine receptor interaction (p=2.01×10^{-12}), staphylococcus aureus infection (p=1.37×10^{-7}), phagosome (p=1.94×10^{-7}) and PI3K-Akt signaling pathway (p=9.74×10^{-6}, Table II). Subsequently, the AEBP1-co-expressed gene-pathway regulatory network was constructed (Figure 4).

Silencing AEBP1 Inhibited the Proliferation of Jurkat Cells

Compared with that in the normal cell line Pbmcs, the expression of AEBP1 was significantly upregulated in Jurkat, Nalm-6, and Raji cells (p<0.05, Figure 5A). Then, AEBP1 was knocked down in Jurkat cells and confirmed by RT-qPCR and Western blotting (Figure 5B and 5C). Following this, the proliferation of Jurkat cells was assessed and found that silencing AEBP1

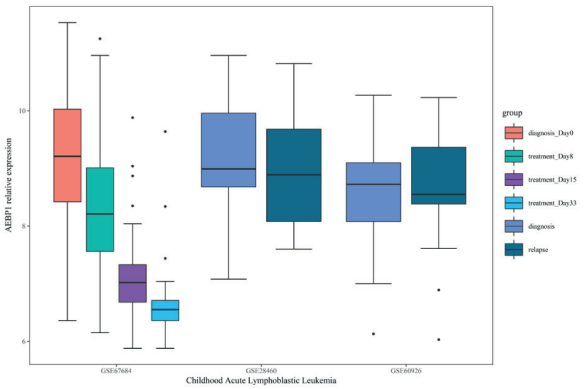

Figure 3. Expression of AEBP1 in different stages of childhood acute lymphoblastic leukemia.

significantly attenuated the proliferation ability of Jurkat cells (Figure 5D).

Silencing AEBP1 Arrested the Cell Cycle of Jurkat Cells

After silencing AEBP1, the cell cycle of Jurkat cells was also analyzed using flow cytometry. The results indicated that percentage of Jurkat cells at the S-stage was significantly lower than that in the control group and the percentage of Jurkat cells at the G1-stage was markedly higher than that in the control group (p<0.01, Figure 6A and 6B). However, no significant difference was identified between these two groups for the G2/M stage. These findings indicated that silencing AEBP1 clearly caused cell cycle arrest of Jurkat cells.

Silencing AEBP1 Increased Cell Apoptosis in Jurkat Cells

Subsequently, apoptosis in Jurkat cells after knocking down AEBP1 was determined. Flow cytometry revealed that silencing AEBP1 significantly increased the apoptosis in Jurkat cells compared with that in the control group (p<0.01, Figure 7A). However, the activity of caspase3/7 was significantly higher in the shAEBP1 group compared with that in the control group (p<0.01, Figure 7B). In addition, the expression levels of p53, Bax, and Bcl-2 were also determined using Western blotting. The results showed that the expression levels of p53 and Bcl-2 were significantly downregulated in the shAEBP1 group

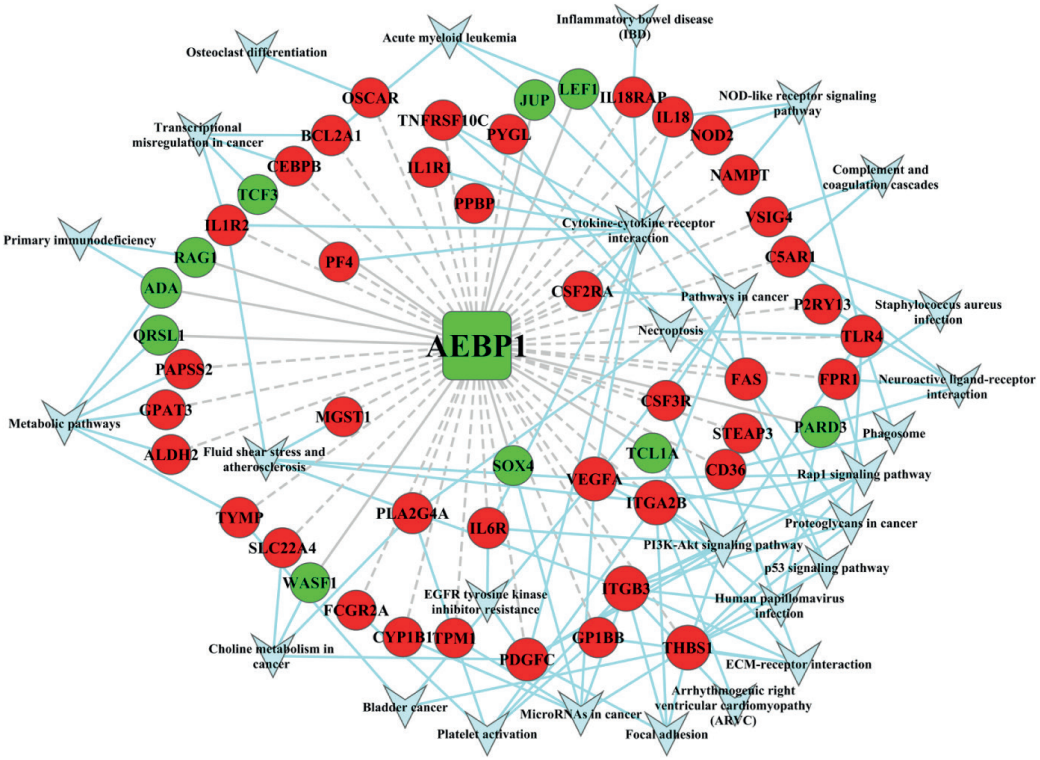

Figure 4. Regulatory network of the AEBP1-co-expressed genes-pathway. The rectangle represents AEBP1, circle represents AEBP1 co-expressed gene, arrow represents gene enriched pathway, red represents the upregulated gene, green represents the downregulated gene, full line represents the positive relationship between AEBP1 and co-expressed gene, and dotted line represents the negative relationship between AEBP1 and co-expressed gene.

Table I. The top 10 GO terms enriched by AEBP1 co-expressed genes.

GO-ID	GO-name	Count	*p*-value	Gene
GO:0006955	Immune response	20	2.73E-18	VPREB1, CEBPB, IL18, CST7, C5AR1, THBS1, RAG1, IL1R1, PF4, CFP ...
GO:0007596	Blood coagulation	18	1.31E-13	F5, ENTPD1, HPS4, PLEK, GP1BB, ITGA2B, PRKAR2B, PF4, PLA2G4A, TREM1 ...
GO:0002576	Platelet degranulation	10	7.65E-13	PPBP, PLEK, PF4, ITGA2B, CLU, VEGFA, F5, CD36, ITGB3, THBS1 ...
GO:0006954	Inflammatory response	14	6.65E-12	IL18RAP, AOAH, CEBPB, CXCR2, CLEC7A, C5AR1, FPR2, THBS1, TNFAIP6, IL18 ...
GO:0007155	Cell adhesion	16	1.50E-11	CD72, TNFAIP6, CSF3R, ITGB3, ITGA2B, CD33, VCAN, THBS1, ADA, COL5A1 ...
GO:0030168	Platelet activation	12	2.20E-11	THBS1, VEGFA, ITGA2B, PPBP, CLU, PLA2G4A, PLEK, PF4, ITGB3, GP1BB ...
GO:0007166	Cell surface receptor signaling pathway	9	1.31E-08	SIRPB1, ANXA1, CLEC1B, GP1BB, IGSF6, CXCR2, IL18RAP, IL1R1, CD36
GO:0044281	Small molecule metabolic process	20	1.39E-07	ADA, UPP1, PRKAR2B, SLC23A1, MGST1, CD36, NAMPT, GPAT3, PAPSS2, KYNU ...
GO:0032760	Positive regulation of tumor necrosis factor production	5	2.82E-07	TLR4, CD36, PF4, NOD2, IL18
GO:0032496	Response to lipopolysaccharide	7	4.76E-07	MGST1, CEBPB, NOD2, C5AR1, TLR4, SLC11A1, TCF3

GO, Gene Ontology.

Table I. The top 10 KEGG pathway enriched by AEBP1 co-expressed genes.

Pathway-ID	Pathway Name	Count	*p*-value	Gene
04640	Hematopoietic cell lineage	11	1.22E-13	IL6R, ITGA2B, ITGB3, IL1R2, CSF2RA, CSF3R, CD33, CD36, IL1R1, DNTT...
04060	Cytokine-cytokine receptor interaction	14	2.01E-12	PF4, IL18, CSF3R, IL1R1, IL6R, CXCR2, PPBP, VEGFA, IL1R2, FAS ...
05150	Staphylococcus aureus infection	6	1.37E-07	PTAFR, C5AR1, FPR1, FPR2, FCAR, FCGR2A
04145	Phagosome	8	1.94E-07	CD36, FCGR2A, ITGB3, FCAR, TUBB1, THBS1, TLR4, CLEC7A
04151	PI3K-Akt signaling pathway	9	9.74E-06	TCL1A, THBS1, TLR4, PDGFC, CSF3R, ITGB3, IL6R, ITGA2B, VEGFA
04380	Osteoclast differentiation	6	1.89E-05	IL1R1, SIRPA, OSCAR, ITGB3, FCGR2A, SIRPB1
01100	Metabolic pathways	16	2.48E-05	NAMPT, RIMKLB, CES1, ADA, GPAT3, KYNU, QRSL1, ALDH5A1, PYGL, ASAH1 ...
04015	Rap1 signaling pathway	7	2.86E-05	ITGB3, PARD3, ITGA2B, PDGFC, THBS1, FPR1, VEGFA
05418	Fluid shear stress and atherosclerosis	6	3.03E-05	ITGA2B, VEGFA, IL1R1, ITGB3, MGST1, IL1R2
04512	ECM-receptor interaction	5	3.34E-05	THBS1, ITGB3, ITGA2B, GP1BB, CD36

KEGG, Kyoto Encyclopedia of Genes and Genomes.

compared with those in the control group, but the expression of Bax was markedly upregulated in the shAEBP1 group compared with that in the control group (Figure 7C). All these findings indicated that knocking down AEBP1 significantly increased apoptosis in Jurkat cells with a p53-dependent pathway.

Discussion

In the present study, three datasets were secondarily mined to identify cALL associated candidates genes. A total of 1621 DEGs were identified in the GSE67684 dataset with two significant gene clusters: profile 1 (downward) and profile 26

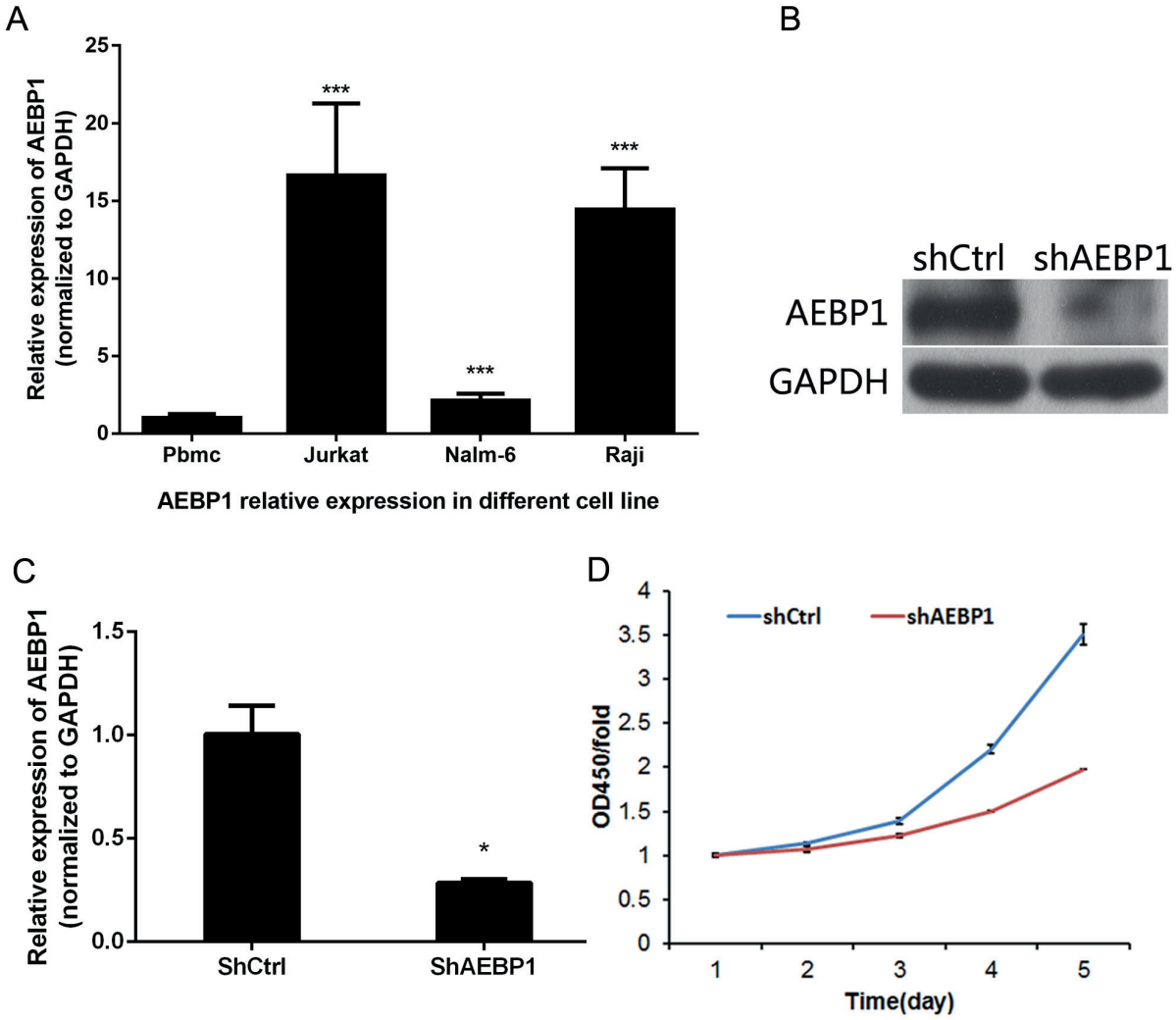

Figure 5. Silencing AEBP1 inhibits the proliferation of Jurkat cells. ***A,*** Relative expression of AEBP1 in leukemia cell lines compared with Pbmc cells (normal control); ***B,*** Silencing AEBP1 confirmed by Western blotting; ***C,*** Silencing AEBP1 validated by quantitative Real-time PCR; ***D,*** Silencing AEBP1 attenuates the proliferation of Jurkat determined by CCK-8 assay. *p<0.05 and *p<0.001 compared with the control group.

(upward). Combined with the DEGs identified in the relapsed datasets GSE28460 and GSE60929, 53 common DEGs were identified in Profile1 and AEBP1 was one of the common DEGs upregulated in cALL. Functional enrichment analysis of AEBP1 co-expressed genes revealed that these genes were significantly enriched in the GO terms such as immune response, blood coagulation, and platelet degranulation and pathways such as hematopoietic cell lineage and PI3K/Akt signaling pathway. In addition, silencing AEBP1 significantly decreased cell proliferation but increase apoptosis of Jurkat cells *via* a p53-dependent pathway. AEBP1 is a ubiquitously expressed protein usually highly expressed in adipose tissue, liver, spleen, lung, and brain[10], but not blood. In the present study, AEBP1 was significantly downregulated in cALL after treatment but markedly upregulated in the relapse cALL. Moreover, Hu et al[11] have demonstrated that the upregulation of AEBP1 drives the resistance of melanoma to BRAF (V600E) inhibition. These findings suggested that upregulation of AEBP1 might be a risk factor for the occurrence and relapse of cALL. Previous investigations[12-14] have demonstrated that AEBP1 plays critical roles in adipogenesis, macrophage cholesterol homeostasis, and inflammatory regulation. In

this study, functional enrichment analysis identified that AEBP1 co-expressed genes were not only significantly enriched in GO terms such as inflammatory response, immune response, and cytokine-cytokine receptor interaction pathways but also markedly enriched in hematopoietic cell lineage, blood coagulation, and platelet degranulation pathways. Considering these lines of evidence, we deduced that AEBP1 can co-operate with its co-expressed genes to modulate the pathogenesis of cALL. To further clarify its biofunction, expression of AEBP1 was determined in lymphoma cell lines and the results indicated that the expression of AEBP1 was significantly upregulated compared with that in normal PBMCs cells, which was consistent with

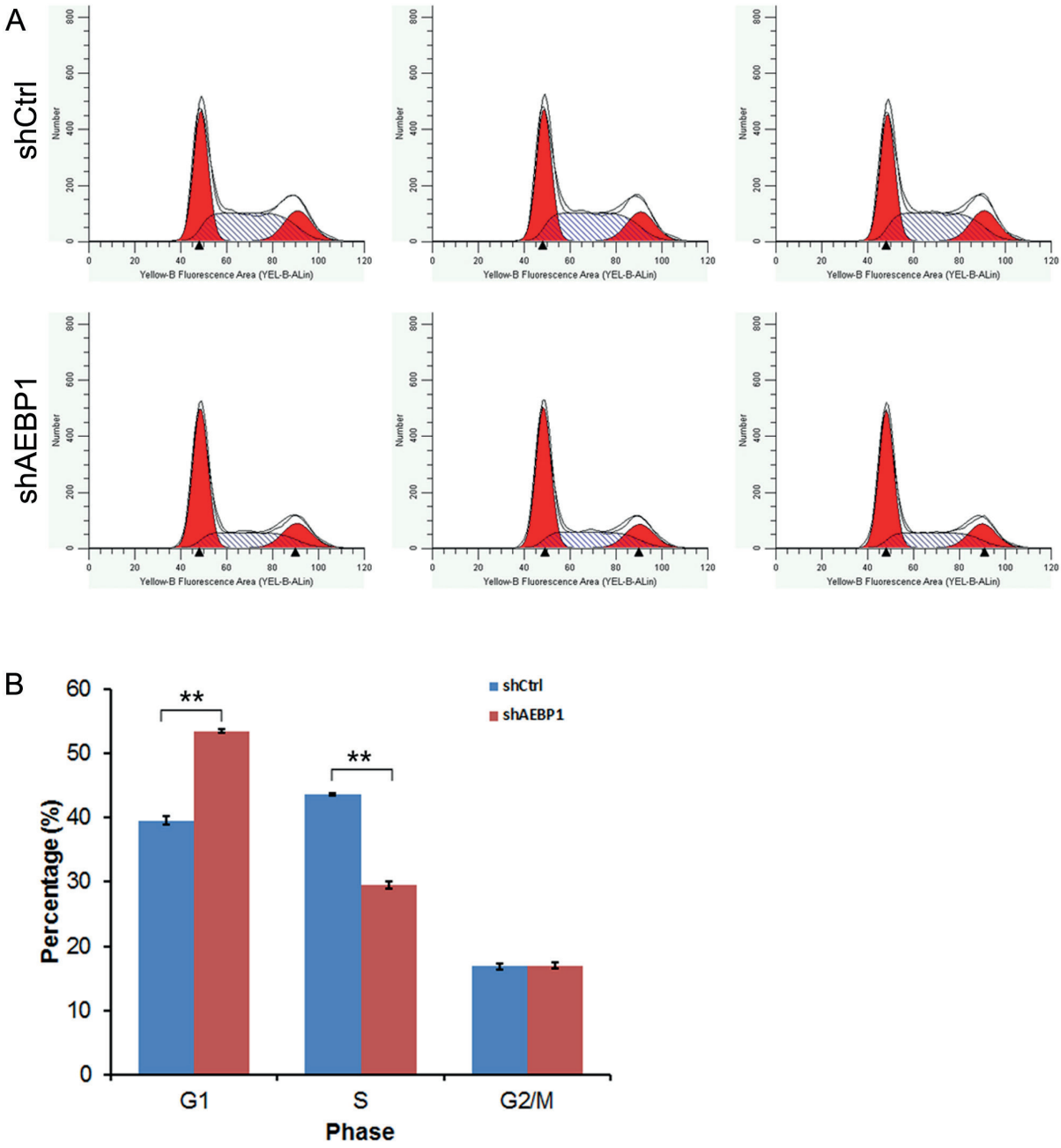

Figure 6. Silencing AEBP1 inhibits cell cycle of Jurkat cells. ***A,*** Cell cycle of Jurkat after silencing AEBP1 determined by flow cytometry; ***B,*** Quantification of Jurkat cell cycle after silencing AEBP1. $^{**}p<0.01$ compared with the control group.

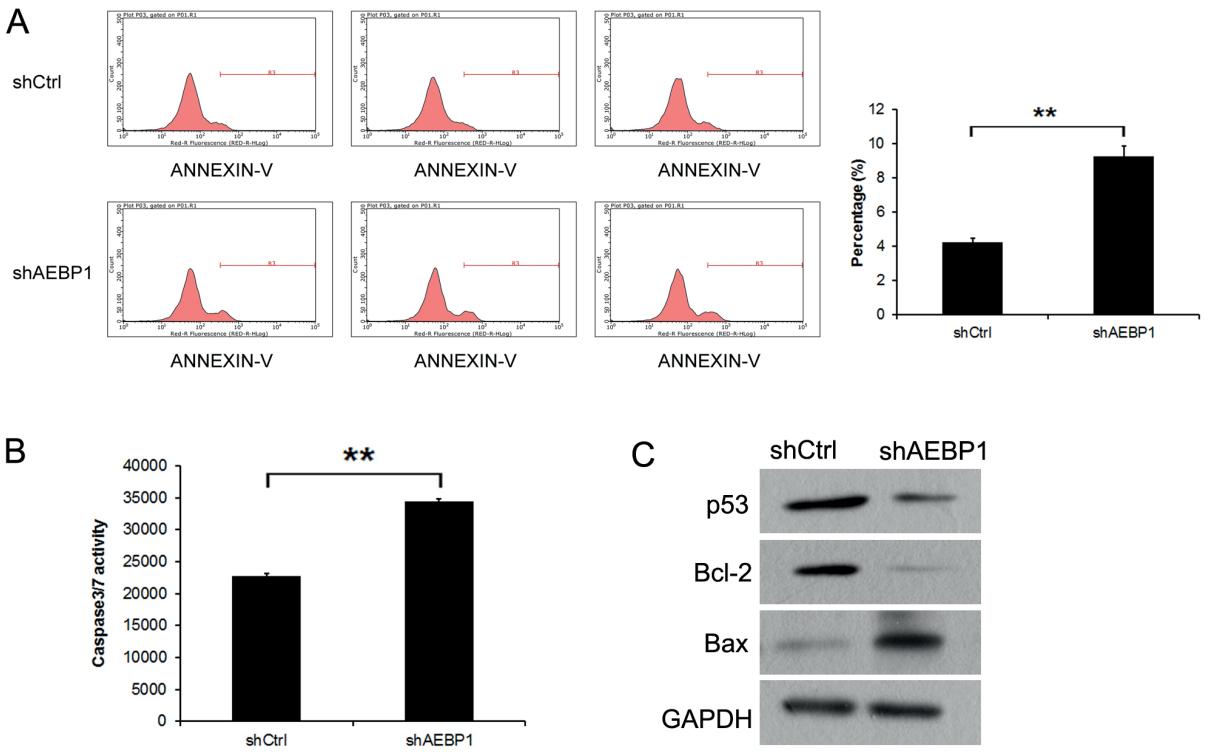

Figure 7. Silencing AEBP1 promotes apoptosis in Jurkat cells. ***A,*** Apoptosis of Jurkat cells after knocking down AEBP1 determined by flow cytometry; ***B,*** Activity of caspase-3/-7 in Jurkat cells after knocking down AEBP1; ***C,*** Expression of p53, Bcl-2, and Bax in Jurkat cells after knocking down AEBP1. $^{**}p<0.01$ compared with the control group.

the bioinformatics findings. Knocking down the expression of AEBP1 significantly inhibited the proliferation and cell cycle of Jurkat cells. Holloway et al[15] have documented that AEBP1 promotes the hyperplasia of mammary epithelial cells *via* proinflammatory and Hedgehog signaling. In addition, the overexpression of AEBP1 was found to result in hyperlipidemia and the development of atherosclerotic lesions in the proximal aortas of mice, whereas the ablation of AEBP1 attenuates the atherosclerosis[16], possibly because it promoted the proliferation and migration of vascular smooth muscle cells[17]. Taken together, AEBP1 might promote the pathogenesis of cALL *via* increasing the proliferation and cell cycle progression in lymphoma cells. However, the exact mechanism of this effect requires to be further clarified. Furthermore, apoptosis in Jurkat cells after silencing AEBP1 was also analyzed and revealing that knockdown of AEBP1 significantly increased apoptosis in Jurkat cells. Researches[18,19] have reported that tumor suppressor p53 is a key protein in suppressing the tumor progression and triggers apoptosis *via* activating the apoptotic effector protein Bax. Bainer *et al*[20] revealed that the p53-regulated apoptotic gene signature could be used to predict the outcome of cALL. Moreover, the germline variation TP53 was also reported to affect the predisposition and prognosis of cALL[21]. Further investigations also found that silencing AEBP1 markedly increased the activity of caspase 3/7 and expression of Bax but decreased the expression of p53 and Bcl-2. Moreover, functional enrichment analysis revealed that ABEP1 associated co-expressed genes were significantly enriched in the PI3K/Akt signaling pathway. Bastian *et al*[22] previously reported that the synergistic activity of botezomib and HDACi regulated the P13K/Akt/p53 and NF-κB signaling pathways to modulate the outcome of B-cell precursor cALL in a preclinical model. Suppipat et al[23] observed that sulforaphane induce cell cycle arrest and apoptosis in ALL via modulating the p53/Akt signaling pathway. Taken together, these findings indicated that AEPB1 might promote proliferation and suppress apoptosis in Jurkat cells via the p53/PI3K/Akt signaling pathway.

Conclusions

AEBP1 was significantly upregulated in the diagnosis and relapse stages of cALL, but markedly reduced after treatment. Moreover, AEBP1 was also significantly upregulated in lymphoma cell lines, especially in Jurkat cells, compared with that in PBMCs. Silencing AEBP1 significantly promoted apoptosis of Jurkat cells and markedly attenuated proliferation and induced cell cycle arrest in Jurkat cells *via* the p53/PI3K/Akt signaling pathway. These findings indicate that AEBP1 might play a critical role in modulating the proliferation and apoptosis of lymphoma cells to regulate the progression of cALL, showing a promising candidate biomarker for the diagnosis and treatment of cALL.

Conflict of Interest

The Authors declare that they have no conflict of interest.

Acknowledgements

This work was supported by grants from the National Natural Science Foundation of China(30872804,81170661 and 31640048 to G.P.Z); Jiangsu Province Science and Education Enhancing Health Project Innovation Team (Leading Talent); Program (CXTDA2017018 toG.P.Z); Nanjing Science and Technology Development Program (201503003 to G.P.Z) and A Project Funded by the Priority Academic Program Development of Jiangsu Higher Education Institutions.

References

1) Hinze L, Moricke A, Zimmermann M, Junk S, Cario G, Dagdan E, Kratz CP, Conter V, Schrappe M, Stanulla M. Prognostic impact of IKZF1 deletions in association with vincristine-dexamethasone pulses during maintenance treatment of childhood acute lymphoblastic leukemia on trial ALL-BFM 95. Leukemia 2017; 31: 1840-1842.
2) Siegel DA, Henley SJ, Li J, Pollack LA, Van Dyne EA, White A. Rates and trends of pediatric acute lymphoblastic leukemia - United States, 2001-2014. MMWR Morb Mortal Wkly Rep 2017; 66: 950-954.
3) Yeoh AE, Tan D, Li CK, Hori H, Tse E, Pui CH. Management of adult and paediatric acute lymphoblastic leukaemia in Asia: resource-stratified guidelines from the Asian Oncology Summit 2013. Lancet Oncol 2013; 14: e508-e523.
4) Qin X, Zhang MY, Liu WJ. Application of minimal residual disease monitoring in pediatric patients with acute lymphoblastic leukemia. Eur Rev Med Pharmacol Sci 2018; 22: 6885-6895.
5) Moorman AV. New and emerging prognostic and predictive genetic biomarkers in B-cell precursor acute lymphoblastic leukemia. Haematologica 2016; 101: 407-416.
6) Livak KJ, Schmittgen TD. Analysis of relative gene expression data using real-time quantitative PCR and the 2(-Delta Delta C(T)) Method. Methods 2001; 25: 402-408.
7) Roberts KG, Morin RD, Zhang J, Hirst M, Zhao Y, Su X, Chen SC, Payne-Turner D, Churchman ML, Harvey RC, Chen X, Kasap C, Yan C, Becksfort J, Finney RP, Teachey DT, Maude SL, Tse K, Moore R, Jones S, Mungall K, Birol I, Edmonson MN, Hu Y, Buetow KE, Chen IM, Carroll WL, Wei L, Ma J, Kleppe M, Levine RL, Garcia-Manero G, Larsen E, Shah NP, Devidas M, Reaman G, Smith M, Paugh SW, Evans WE, Grupp SA, Jeha S, Pui CH, Gerhard DS, Downing JR, Willman CL, Loh M, Hunger SP, Marra MA, Mullighan CG. Genetic alterations activating kinase and cytokine receptor signaling in high-risk acute lymphoblastic leukemia. Cancer Cell 2012; 22: 153-166.
8) Perez-Andreu V, Roberts KG, Harvey RC, Yang W, Cheng C, Pei D, Xu H, Gastier-Foster J, E S, Lim JY, Chen IM, Fan Y, Devidas M, Borowitz MJ, Smith C, Neale G, Burchard EG, Torgerson DG, Klussmann FA, Villagran CR, Winick NJ, Camitta BM, Raetz E, Wood B, Yue F, Carroll WL, Larsen E, Bowman WP, Loh ML, Dean M, Bhojwani D, Pui CH, Evans WE, Relling MV, Hunger SP, Willman CL, Mullighan CG, Yang JJ. Inherited GATA3 variants are associated with Ph-like childhood acute lymphoblastic leukemia and risk of relapse. Nat Genet 2013; 45: 1494-1498.
9) Bandapalli OR, Schuessele S, Kunz JB, Rausch T, Stutz AM, Tal N, Geron I, Gershman N, Izraeli S, Eilers J, Vaezipour N, Kirschner-Schwabe R, Hof J, von Stackelberg A, Schrappe M, Stanulla M, Zimmermann M, Koehler R, Avigad S, Handgretinger R, Frismantas V, Bourquin JP, Bornhauser B, Korbel JO, Muckenthaler MU, Kulozik AE. The activating STAT5B N642H mutation is a common abnormality in pediatric T-cell acute lymphoblastic leukemia and confers a higher risk of relapse. Haematologica 2014; 99: e188-e192.
10) Ro HS, Kim SW, Wu D, Webber C, Nicholson TE. Gene structure and expression of the mouse adipocyte enhancer-binding protein. Gene 2001; 280: 123-133.
11) Hu W, Jin L, Jiang CC, Long GV, Scolyer RA, Wu Q, Zhang XD, Mei Y, Wu M. AEBP1 upregulation confers acquired resistance to BRAF (V600E) inhibition in melanoma. Cell Death Dis 2013; 4: e914.
12) Majdalawieh A, Zhang L, Fuki IV, Rader DJ, Ro HS. Adipocyte enhancer-binding protein 1 is a potential novel atherogenic factor involved in macrophage cholesterol homeostasis and inflammation. Proc Natl Acad Sci U S A 2006; 103: 2346-2351.
13) Majdalawieh A, Ro HS. PPARgamma1 and LXRalpha face a new regulator of macrophage choles-

terol homeostasis and inflammatory responsiveness, AEBP1. Nucl Recept Signal 2010; 8: e4.

14) Majdalawieh A, Ro HS. Regulation of IkappaBalpha function and NF-kappaB signaling: AEBP1 is a novel proinflammatory mediator in macrophages. Mediators Inflamm 2010; 2010: 823821.

15) Holloway RW, Bogachev O, Bharadwaj AG, McCluskey GD, Majdalawieh AF, Zhang L, Ro HS. Stromal adipocyte enhancer-binding protein (AEBP1) promotes mammary epithelial cell hyperplasia via proinflammatory and hedgehog signaling. J Biol Chem 2012; 287: 39171-39181.

16) Bogachev O, Majdalawieh A, Pan X, Zhang L, Ro HS. Adipocyte enhancer-binding protein 1 (AEBP1) (a novel macrophage proinflammatory mediator) overexpression promotes and ablation attenuates atherosclerosis in ApoE (-/-) and LDLR (-/-) mice. Mol Med 2011; 17: 1056-1064.

17) Bennett MR, Sinha S, Owens GK. Vascular smooth muscle cells in atherosclerosis. Circ Res 2016; 118: 692-702.

18) Follis AV, Llambi F, Merritt P, Chipuk JE, Green DR, Kriwacki RW. Pin1-induced proline isomerization in cytosolic p53 mediates bax activation and apoptosis. Mol Cell 2015; 59: 677-684.

19) Giorgi C, Bonora M, Sorrentino G, Missiroli S, Poletti F, Suski JM, Galindo RF, Rizzuto R, Di Virgilio F, Zito E, Pandolfi PP, Wieckowski MR, Mammano F, Del SG, Pinton P. p53 at the endoplasmic reticulum regulates apoptosis in a Ca2+-dependent manner. Proc Natl Acad Sci U S A 2015; 112: 1779-1784.

20) Bainer RO, Trendowski MR, Cheng C, Pei D, Yang W, Paugh SW, Goss KH, Skol AD, Pavlidis P, Pui CH, Gilliam TC, Evans WE, Onel K. A p53-regulated apoptotic gene signature predicts treatment response and outcome in pediatric acute lymphoblastic leukemia. Cancer Manag Res 2017; 9: 397-410.

21) Qian M, Cao X, Devidas M, Yang W, Cheng C, Dai Y, Carroll A, Heerema NA, Zhang H, Moriyama T, Gastier-Foster JM, Xu H, Raetz E, Larsen E, Winick N, Bowman WP, Martin PL, Mardis ER, Fulton R, Zambetti G, Borowitz M, Wood B, Nichols KE, Carroll WL, Pui CH, Mulligan CG, Evans WE, Hunger SP, Relling MV, Loh ML, Yang JJ. TP53 germline variations influence the predisposition and prognosis of B-cell acute lymphoblastic leukemia in children. J Clin Oncol 2018; 36: 591-599.

22) Bastian L, Hof J, Pfau M, Fichtner I, Eckert C, Henze G, Prada J, von Stackelberg A, Seeger K, Shalapour S. Synergistic activity of bortezomib and HDACi in preclinical models of B-cell precursor acute lymphoblastic leukemia via modulation of p53, PI3K/AKT, and NF-kappaB. Clin Cancer Res 2013; 19: 1445-1457.

23) Suppipat K, Park CS, Shen Y, Zhu X, Lacorazza HD. Sulforaphane induces cell cycle arrest and apoptosis in acute lymphoblastic leukemia cells. PLoS One 2012; 7: e51251.